

Performance of the first HAWAII 4RG-15 arrays in the laboratory and at the telescope

Donald N. B. Hall¹, Dani Atkinson¹, James W. Beletic², Richard Blank², Mark Farris², Klaus W. Hodapp¹,
Shane M. Jacobson¹, Markus Loose³, and Gerard Luppino⁴

¹University of Hawaii, Institute for Astronomy, 640 North A'ohoku Place, Hilo, HI 96720, USA

²Teledyne Imaging Sensors, 5212 Verdugo Way, Camarillo, CA 93012, USA

³Markury Scientific, 518 Oakhampton Street, Thousand Oaks, CA 91362, USA

⁴GL Scientific, 3367 Waialae Ave, Honolulu, HI 96816, USA

ABSTRACT

The primary goal of the HAWAII 4RG-15 (H4RG-15) development is to provide a 16 megapixel 4096x4096 format at significantly reduced price per pixel while maintaining the superb low background performance of the HAWAII 2RG (H2RG). The H4RG-15 design incorporates several new features, notably clocked reference output and interleaved reference pixel readout, that promise to significantly improve noise performance while the reduction in pixel pitch from 18 to 15 microns should improve transimpedance gain although at the expense of some degradation in full well and crosstalk. During the Phase-1 development, Teledyne has produced and screen tested six hybrid arrays. In preparation for Phase-2, the most promising of these are being extensively characterized in the University of Hawaii's (UH) ULBCam test facility originally developed for the JWST H2RG program. The end-to-end performance of the most promising array has been directly established through astronomical imaging observations at the UH 88-inch telescope on Mauna Kea. We report the performance of these Phase-1 H4RG-15s within the context of established H2RG performance for key parameters (primarily CDS read noise), also highlighting the improvements from the new readout modes.

Keywords: HgCdTe detector array, H4RG-15 ROIC, hybrid CMOS, large format, HAWAII, 4k x 4k

1. INTRODUCTION

The development of the HAWAII 4RG-15 (H4RG-15) continues the management approach used by the University of Hawaii (UH) – Rockwell Scientific Company (RSC) academic- industrial partnership in the successful development of the HAWAII family of HgCdTe arrays (HAWAII 1 & 2, 1R and 1RG & 2RG) and the SIDECAR ASIC for NASA. Within this partnership UH is both the proposing institution and the recipient of the award with ultimate overall responsibility for its execution; UH has specifically provided scientific leadership, representing the interests of the science user community, and unique test capabilities, both at low background in the laboratory and at telescopes on Mauna Kea. The H4RG-15 is being developed for the NSF primarily for ground based astronomy applications – the HAWAII arrays are widely used for these at telescopes around the world and the H2RG is generally regarded as the array of choice for ground based observations in the 1 to 5.5 μm wavelength interval - and RSC has become Teledyne Imaging Sensors (TIS) with its acquisition by Teledyne Technologies Incorporated (TTI) in 2006; Gerry Luppino, who originally participated as a UH faculty member, is now involved through GL Scientific.

The H4RG-15 development at TIS is separated into two phases – an initial prototyping phase (Phase-1) followed by a pilot production phase (Phase-2); this is more fully described in a companion paper ⁽¹⁾. As originally envisaged in the proposal, the Phase-1 test program at UH had one very specific goal: to evaluate H4RG-15 readouts (ROICs) produced by TIS' proven HxRG silicon foundry, United Microelectronics Corporation (UMC) located in Hsinchu Taiwan. This utilized both stand-alone bare ROICs and also those incorporated into H4RG-15 hybrid arrays (sensor chip assemblies or SCAs), aiming to demonstrate that performance at least equals the established performance of the now thoroughly characterized H2RG. The intent is not to establish baseline performance (this task is better done with Phase-2 SCAs) but rather to focus on areas such as pixel pitch, array format and the new column de-select feature which involve changes

from the H2RG to the H4RG-15. However, despite being tightly cost and schedule constrained (cost to allow maximum allocation of resources to the TIS prototyping effort and schedule in order to move on to Phase-2 at TIS) the UH test program has been expanded to encompass two additional primary goals, i.e. to: 1) evaluate the performance at cryogenic temperatures of H4RG-15 ROICS and SCAs produced by a new silicon foundry, ON Semiconductor, located in Gresham Oregon and, 2) bring up and evaluate new features not available in the H2RG, notably Interleaved Reference Pixel (IRP) readout mode and a clocked reference output. In a significant setback, UH was unable to bring up a conventional 64+ channel controller (the 64+ allows for unspecified additional channels to accommodate the guide and reference outputs and other options) in time for the Phase-1 testing and a SIDECAR ASIC operated in 32 channel mode was, of necessity, substituted.

Based on TIS' screening tests as described in the companion paper ⁽¹⁾, the most promising UMC and ON SCAs were first shipped to UH and installed on November 12 (UMC) and December 31 (ON), 2011 for comprehensive evaluation, particularly of CDS read noise. This was targeted to the eventual selection of one or the other for direct imaging characterization at the UH 88-inch telescope on Mauna Kea. The overall UH laboratory test program, the specific CDS noise investigation, the effectiveness of the new IRP readout mode and the imaging observations at the telescope are reported in the sections below.

2. OVERVIEW OF THE UH LABORATORY TEST PROGRAM

All of the UH laboratory characterization of Phase-1 H4RG-15 SCA's has utilized the ULBCam test facility ⁽²⁾ (Figure 2.1) originally developed for both laboratory and telescope evaluation of the 2 x 2 H2RG prototype of NASA's JWST NIRCam mosaic focal plane. ULBCam has higher background, particularly in the telescope mode, than the KSPEC test facility ⁽³⁾ used for the ultra-low background characterization of the JWST Packaging and Manufacturing Technology (P&MT) SCA's but the level is entirely adequate for the Phase-1 H4RG-15 SCAs utilize 2.5 μm (rather than 5.5 μm) cutoff MBE material. Use of ULBCam in telescope mode throughout the Phase-1 laboratory test program allowed rapid

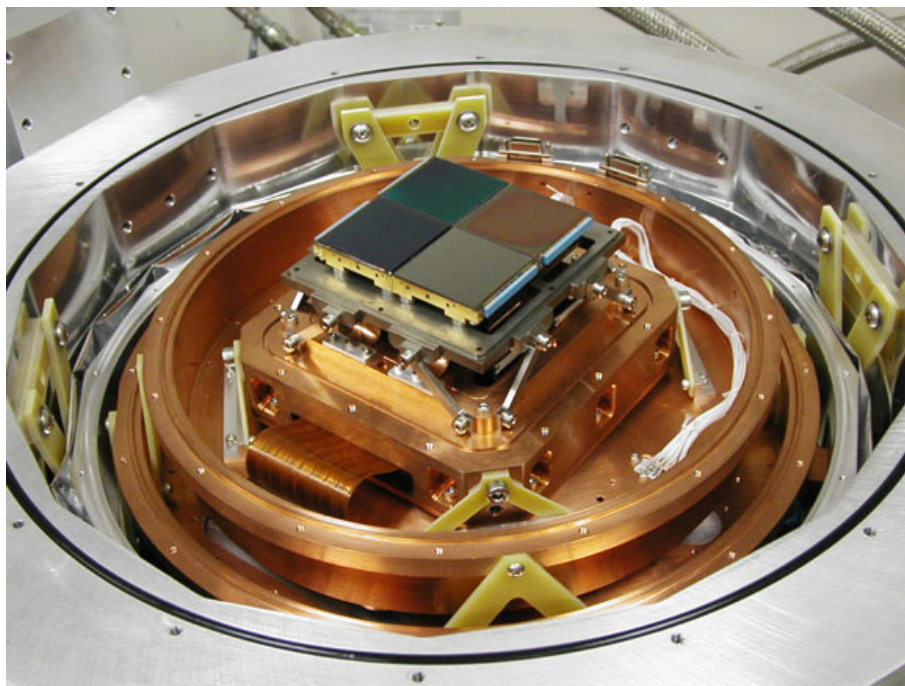


Figure 2.1: The JWST NIRCam-like 2 x 2 mosaic of H2RG SCAs mounted in ULBCam. The slightly smaller H4RG-15 SCA mounts to the same base-plate through a SiC attachment assembly.

Change over between ultra-low background noise tests (with a cold blank-off) and ramps up to full well with illumination through either J or H filters.

The entire Phase-1 test program at UH has utilized a SIDECAR ASIC operating at the same cryogenic temperature as the H4RG-15 SCA. While SIDECAR operation is ideal for many space applications which place a premium on low power consumption along with the immunity to RFI offered by the proximity of the ASIC controller to the SCA, it is less satisfactory for initial characterization of a new SCA, primarily because of the lack of access to the clocks, power supplies and signal lines between the controller and the SCA. This necessitates delicate fine tuning of the ASIC controller and the H4RG-15 SCA as an integrated system rather than optimizing each separately and prevents direct separation of noise sources. However within these constraints, the UH team was able to achieve all of the Phase-1 test program objectives and is committed to conducting the Phase-2 program with a fully optimized conventional 64+ channel controller.

The UH Phase-1 laboratory test program has focused almost exclusively on the limiting CDS read noise of both H4RG-15 bare ROICs and SCAs and on the new IRP readout capability. The first was driven by the need to retire the risk of a ROIC re-design and foundry run before moving on to Phase-2 while the IRP readout was emphasized because of its potential to greatly mitigate many of the excess noise sources and performance limiting traits of the ASIC. Both were critical to qualifying the ON readout as it had not previously been characterized to astronomy standards at cryogenic temperatures.

In these tests the rms CDS voltage noise (in rms μV) was evaluated for both UMC and ON readouts against the established “benchmark” performance of the H2RG. The rms voltage noise is preferred over the commonly used (in astronomy) rms charge noise (in rms e-) for direct comparison of intrinsic ROIC readnoise because in CMOS source-follower charge-integrating readouts it is the parameter that is directly measured and calibrated (it is also first order independent of the dimensions of the gate of the input MOSFET - often driven by pixel pitch). The corresponding charge noise is then set by the node capacitance (which must be measured by procedures that involve significant correction factors ⁽⁴⁾); further, the node capacitance, and hence the charge gain, varies substantially with photodiode bias. The best voltage noise values measured for the H2RG should then provide a “benchmark” value that can be used as a yardstick for the H4RG-15. The lowest published values for the H2RG single CDS voltage noise at 100 kHz pixel read rate all cluster around 40 rms μV for the embedded perimeter reference pixels and also for a few outstanding SCAs. Gert Finger for SN 49 and SN 88 ⁽⁴⁾ and Roger Smith for SNAP H2RG SCAs ⁽⁵⁾ both report 8.2 rms e- corresponding to 40 rms μV for a node capacitance of 33 fF and Don Hall reports ⁽⁶⁾ 40 μV for JWST P&MT H2RGs. Active pixels generally exhibit substantial excess noise – Gert Finger reports ⁽⁴⁾ 60 to 80 μV for the Hawk-I H2RGs while Roger Smith ⁽⁵⁾ reports 135 μV for the 1.7 μm cutoff SNAP arrays. However a few 2.5 μm cutoff H2RGs do have active pixel noise comparable to the reference pixel value - Gert Finger has reported 40 μV for the signal pixels in one such H2RG, SN 49. Simulations of the readnoise in the H4RG-15 ROIC predict a very similar value of 38 rms μV . For the projected H4RG-15 node capacitance of 27 fF, the predicted conversion gain is 6 $\mu\text{V}/\text{e-}$ i.e. a “benchmark” charge read noise of 6.5 rms e-.

3. UH CDS NOISE ETC. CHARACTERIZATION

The UH Phase-1 CDS noise evaluation has been closely focused on measurements that characterize CDS noise as a function of two variables: FNDELTA, the number of data ramp frames between the two frames subtracted to form the CDS frame, and 2) FNAVG, the number of CDS frames at this FNDELTA averaged to form the final frame for noise analysis (Figure 3.1). A standard data ramp consists of two pixel-by-pixel resets followed by a modest number of drop frames (typically eight) to settle the array before the 256 data frames. The relatively large number of drop frames would be a significant penalty in actual astronomical observations but has the significant advantage for the current readnoise evaluation of facilitating temporal noise analysis where the noise is calculated independently for each pixel from the time sequence of values up the ramp. This is more rigorous than spatial noise analysis which evaluates the noise using relative values within spatial ensembles of pixels.

Having experimentally determined that there is no significant change in readnoise from 100 kHz to 200 kHz pixel readout rate for the H4RG-15, 200 kHz has been used for the standard noise comparison tests. With the H4RG-15 SCA operated in 32 output mode, this results in a 2.7 second frame time in conventional readout mode and a 5.4 second frame time in IRP readout mode. The 256 frame ramps simulate up to 10 (or 20) minute duration data sets with up to 350 (or 700) second exposure times representative of those used in ground based astronomy. Dark current is not an issue for

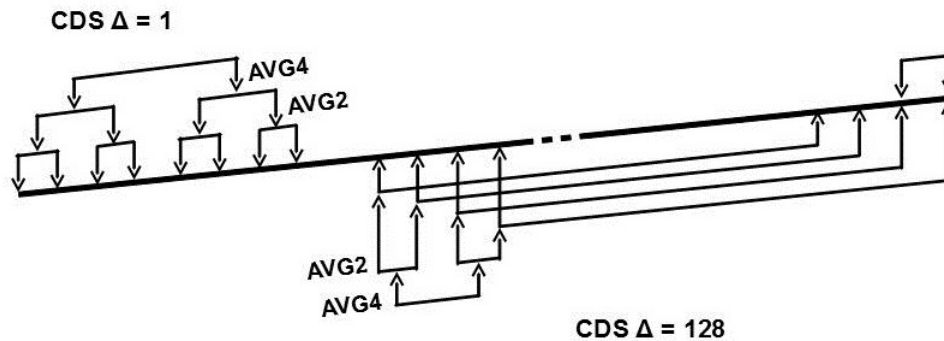


Figure 3.1: Illustration of low order CDS averaging with frame delta of 1 and 128 for a 256 frame ramp.

noise measurements using the embedded perimeter reference pixels but needs to be kept down around an electron per thousand seconds (e-/ksec) to avoid biasing extreme FAVG noise measurements. Our dark current measurement limit with ULBCam in telescope configuration is a few e-/ksec; we were able to achieve this for a significant number of pixels for operating temperatures as high as 80K with a significant reduction in hot pixel count as temperature was reduced to 60K (Figure 3.2). As there was no significant change in readnoise for the “good” pixels over the 60 to 80K range, all of the data used in the CDS readnoise comparison was taken at 60K.

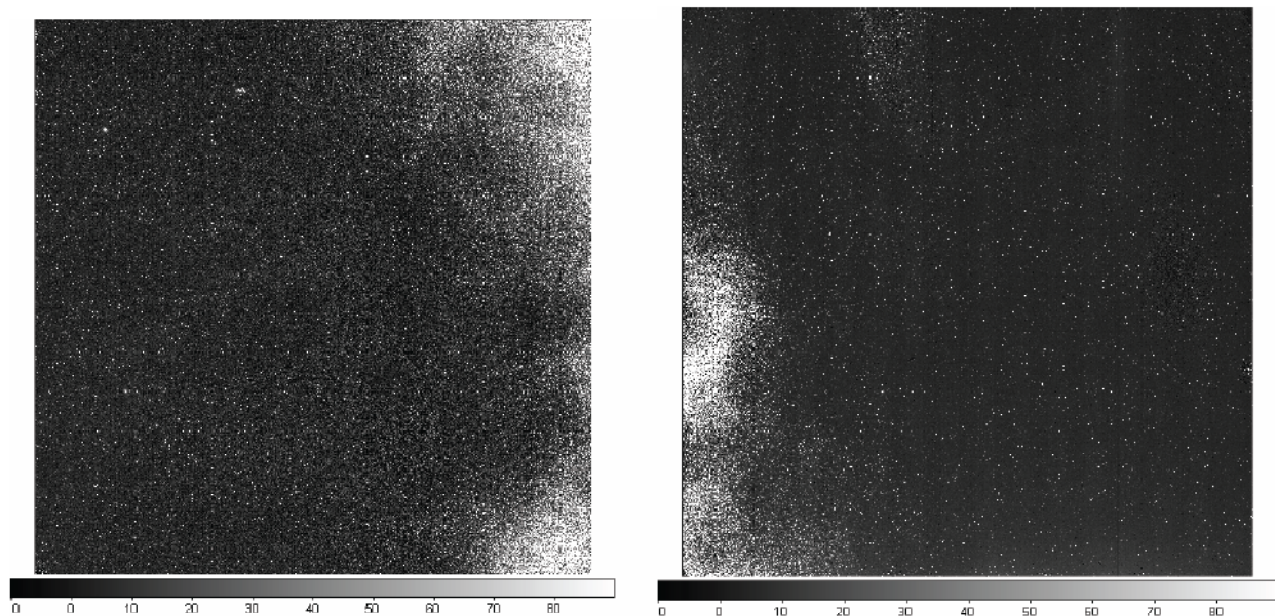


Figure 3.2: Dark current at 60K in the UMC (left) and ON (right) SCAs.

The similarity of the readnoise at 100 kHz and 200 kHz pixel read rates, although counter-intuitive, has been widely reported. The pixel readout is very sparsely sampled (once per frame corresponding to a 1:500,000 duty cycle for 32output operation) and the result is consistent with the noise bandwidth being limited to a value lower than the respective 50 kHz and 100 kHz Nyquist frequencies somewhere else in the signal chain. This effect has not been further pursued as part of the current investigation.

Each 128 column x 4096 row output “stripe” is treated independently in the noise analysis. The mean, median and modal noise is computed for the 256 values (one per frame) for every pixel in the stripe that satisfies certain masking criteria (voltage immediately after reset within a proscribed range, dark current below a proscribed value etc.). The vertical

(column) perimeter reference pixels are excluded from the analysis (to avoid biasing the noise estimates) and the averages of the top and bottom horizontal (row) perimeter reference pixels in each stripe are used to correct long term DC drifts. The average noise values for signal and embedded horizontal reference pixels are computed for each stripe; the median noise is the parameter used in the noise comparison analysis.

After initial verification that for $FNAVG = 1$, there was no significant variation in CDS median noise with $FNDELTA$ for values increasing in powers of two from 1 to 128 (Figure 3.3), the noise comparison has focused on $FNAVG$ values

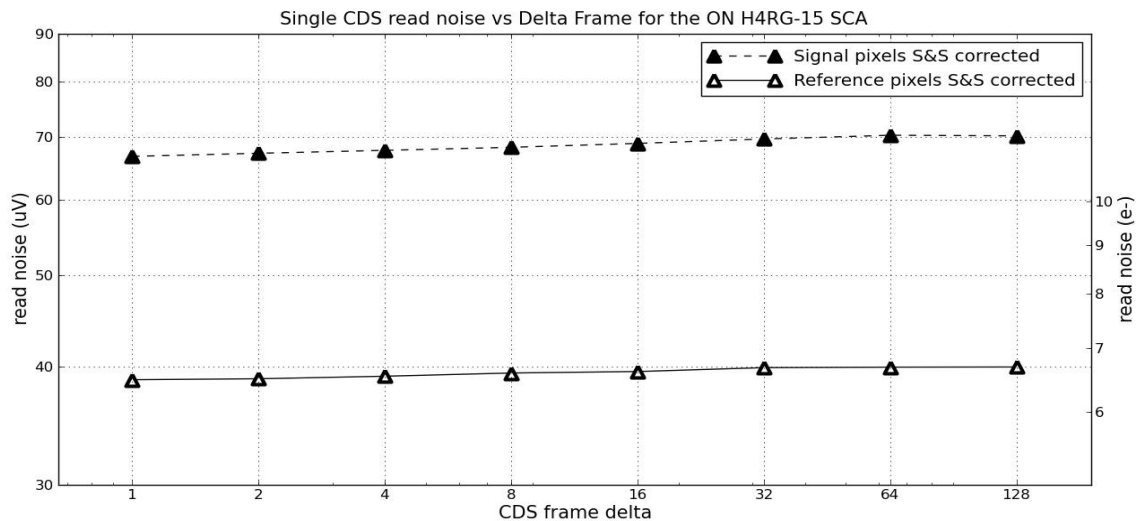


Figure 3.3: Single CDS noise as a function of frame delta for the ON SCA. The trend is statistically significant but at a level negligible with respect to other noise trends.

of 1, 2, 4, 8 and 16 for the case $FNDELTA = 128$ (using only data from a single ramp, higher CDS averages do not involve enough values to be statistically significant). Typically five ramps are run with the first “settling” ramp being discarded and the last one, two or four ramps used in the analysis. We have also accumulated 33 ramp sets for each H4RG-15 SCA to extend the noise comparison $FNAVG$ values of 32, 64 and 128 and have completed some preliminary analysis for $FNAVG = 128$. However these data are very preliminary as, particularly for the reference pixels, the CDS $FNAVG = 128$ noise values are below 10 rms μV (i.e. approaching 1 rms e^-) where digitization becomes significant and discrete electron jumps in dark current may also bias the statistics.

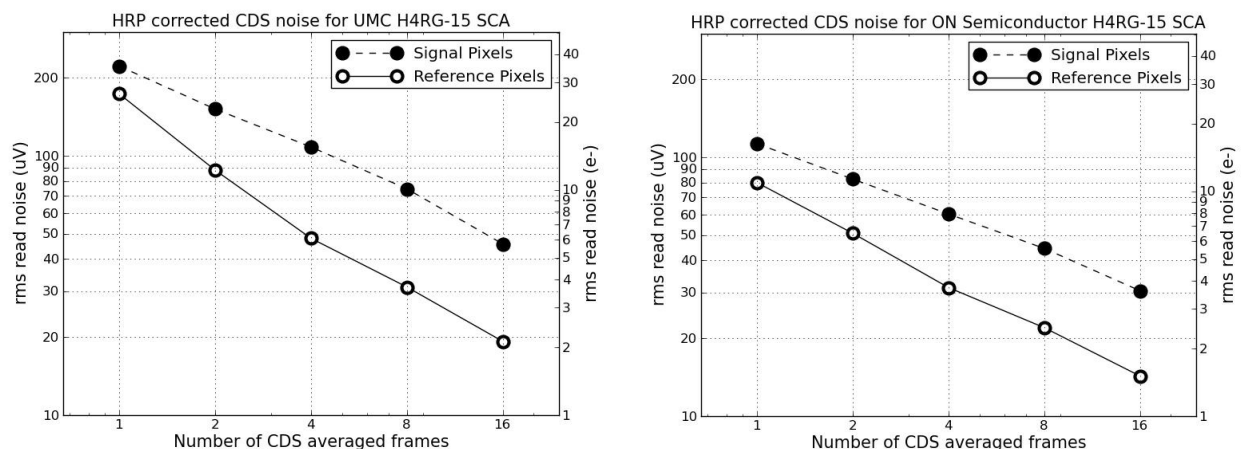


Figure 3.4: CDS noise from frames corrected only with the average of the horizontal reference pixels. Vertical reference pixel correction, not used because it biases noise measurements, does not significantly improve these values.

CDS noise data were first acquired and analyzed for the UMC H4RG-15 SCA as its noise performance could be directly referenced to the H2RG database. The median CDS averaged noise values for the signal and reference pixels (Figure 3.4) are disappointing – they are far higher than the benchmark and do not average down approximately as $\text{SQRT}[\text{FNAVG}]$. This is usually an indicator of excess noise correlated between frames. Because for Phase-1 we are interested primarily in comparing the intrinsic ROIC input noise, rather than having to beat down the noise during actual observations, we have used the “shift-and-subtract” (S&S) technique to reject common mode noise. This involves subtracting the value for each pixel from the one shifted 256 columns (exactly two “stripes” – the pixel read out simultaneously by the next readout but one). The shift needs to be two, rather than one, stripe because, in a holdover from NASA’s JWST requirements, the SIDECAR ASIC is set by default to read successive outputs in opposite scan directions. S&S will cancel common mode noise but not the noise unique to the output (i.e. the unit cell and output source followers) while adding in quadrature all uncorrelated noise sources. If the latter are of equal magnitude in the two outputs then the

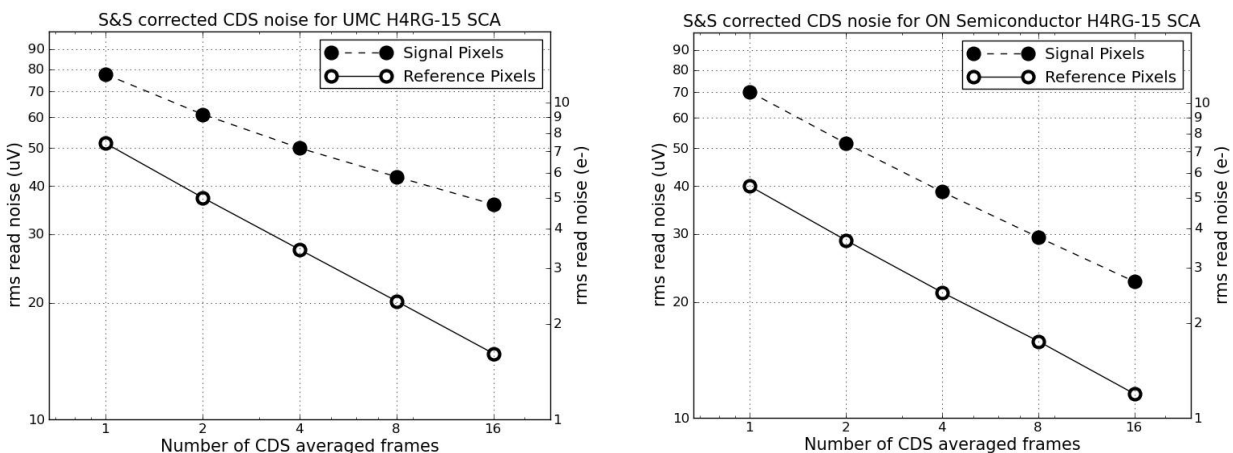


Figure 3.5: The CDS read noise is lowered dramatically with S&S, closely approximating $1/\text{SQRT}[N]$ dependence.

noise power is doubled and the intrinsic noise can be estimated by dividing the observed noise amplitude by $\text{SQRT}[2]$. S&S median noise values, scaled by $\text{SQRT}[2]$, for the UMC H4RG-15 SCA are shown in Figure 3.5. Two major improvements are evident: 1) the rms median noise in the reference pixels is reduced to a level approaching the H2RG benchmark, and 2) the noise in the signal and particularly the reference pixels decreases as $\text{FNAVG}^{(-1/2)}$. The equivalent results for the ON Semiconductor H4RG-15 SCA are shown in Figures 3.3c & d. The ON SCA exhibits the same improvement with S&S but with a lower noise that closely matches the H2RG benchmark value. The stability of the

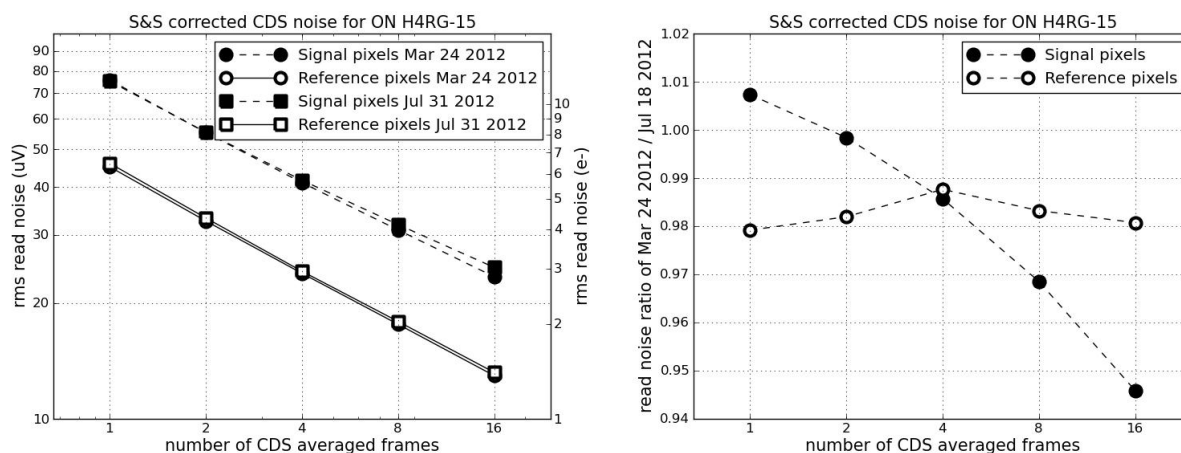


Figure 3.6: The excellent agreement between S&S corrected and IRP readout CDS noise. As the discrepancies are more pronounced for the signal pixels, they are likely attributable to shortcomings in the masking of the Phase-1 SCAs.

noise measurements for the ON H4RG-15 SCA is demonstrated in Figure 3.6 which compares data taken in April with two sets taken in July, the SCA having been transported to Mauna Kea and back and then removed and re-installed with the control software upgraded in the interim. The important result is that for even these Phase-1 parts with high current draw, both the UMC and ON H4RG-15 SCAs achieve rms voltage noise performance comparable to the best results reported for the H2RG and they are both entirely viable candidates for further characterization at the telescope. The reduction in node capacitance associated with the reduction in pixel pitch from 18 to 15 μm should translate into a modest, but significant, reduction in the corresponding rms charge noise. The difference in CDS noise between these specific UMC and ON parts is firmly established. However it would be premature to draw any conclusions about the relative merits of the two foundries from just these two Phase-1 parts, both of which incorporate ROICs with high current draw.

We have also made a preliminary assessment of readout glow. This is primarily associated with photons emitted by the readout and detected by the HgCdTe – it is expressed in e- per read in contrast to dark current expressed in e-/sec. We have assessed the glow level in the H4RG-15 by comparing: 1) a CDS [320,320] subtracted image from a 640 frame, 1,000 second exposure ramp taken without IRP correction with, 2) a CDS [64,64] subtracted image from a 128 frame, 1,000 second exposure ramp, also without IRP correction. Both CDS frames (Figure 3.7) have the same 1,000 second dark current contribution. This cancels when they are subtracted, leaving only the glow contribution associated with 256 reads.

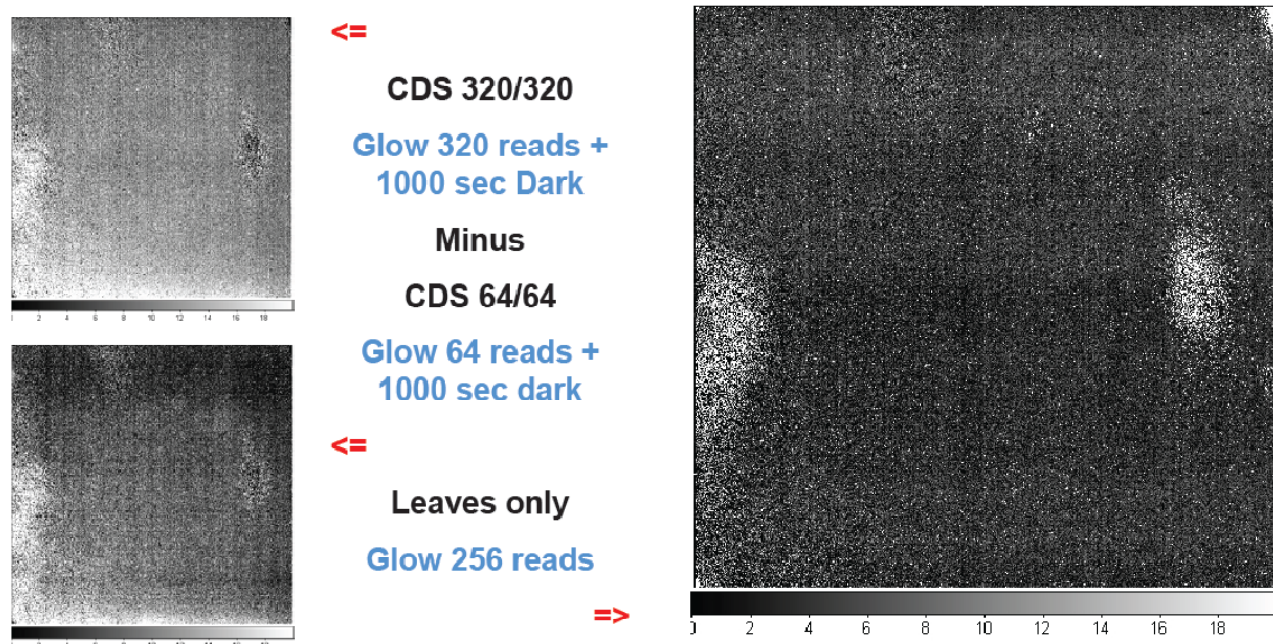


Figure 3.7: The dark current subtracted “glow” frame (right) exhibits no discernible structure.

This data, also shown in Figure 3.7 allow us to place a limit of <1 e- per 50 reads on uniform glow and the absence of any spatial structure at <1 e- per 250 reads suggests the unit cell as the source of any uniformly distributed residual glow (although data from improved Phase-2 SCAs will be required to confirm the existence of this). The level of 1 e- per 50 reads is already acceptable for most astronomical applications and, as the glow should drop exponentially with unit cell source current, we have deferred more detailed investigation until Phase-2.

4. INTERLEAVED REFERENCE PIXEL READOUT

IRP readout and the clocked reference output are additional features of the H4RG-15 that are not available in either the H2RG or earlier HAWAII arrays. As described in Section 1.1 of the companion paper ⁽¹⁾, both utilize separate rows of reference pixels, located between the body of the array and the outputs, which are clocked in sync with the row being read out from the science array. To generate the parallel reference output the reference pixel in the same column as selected for output 0 is read out through a dedicated reference output (RefOut) channel while for IRP readout mode all

outputs are toggled between the row being read out and the reference row to read out a reference pixel immediately following all or selected active pixels. Although not clocked, the reference output of the H2RG has been used to advantage in sophisticated post-processing noise reduction ⁽⁷⁾. However as the new clocked reference output of the H4RG-15 was not of obvious benefit for UH's Phase-1 test program, it has not been investigated beyond verification of functionality. In contrast, the IRP readout mode was seen as having major potential benefits for noise suppression along with common mode rejection of RFI at the telescope. Accordingly significant resources were devoted to prototyping software to allow integral use of the IRP readout capability (in its simplest form) for both noise characterization in the laboratory and also imaging of astronomical sources with the UH 88-inch telescope.

For the Phase-1 UH program Markury Scientific implemented prototype IRP data acquisition software to simply read out an interleaved reference pixel immediately following the readout of each active pixel with the reference pixel values stored in a second 4096 x 4096 reference frame. Direct subtraction of this IRP reference frame from its active pixel equivalent generates a CDS frame analogous to the familiar CCD readout. For the Phase-1 program we were prepared to accept the noise penalties that come with this approach i.e. 1) the exposure time to record the same number signal or CDS frames is doubled with a noise penalty of $\text{SQRT}[2]$, and 2) the reference pixel readnoise is added in quadrature with that of the active pixels, another noise penalty of up to $\text{SQRT}[2]$ (depending on the level of excess noise in the active pixels). Both of these penalties can be mitigated through the use of more sophisticated IRP readout sequences that more sparsely sample the reference pixels while apodizing the reference subtract value from a weighted running average of reference pixels. Note that the first of these requires modifications to the data acquisition sequence while the second involves only re-processing of the existing data.

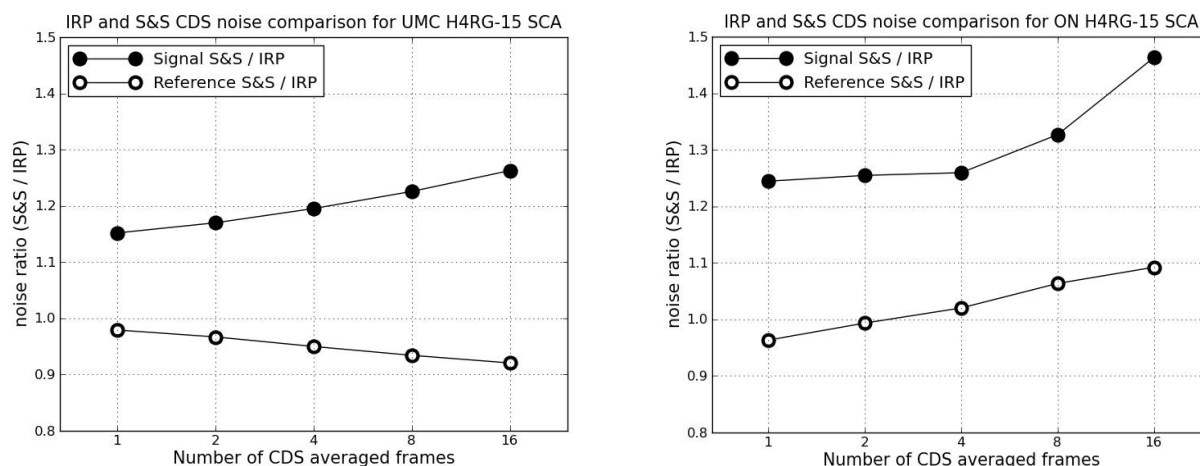


Figure 4.1: The reduction in read noise achieved by the application of interleaved reference pixels in comparison to that of the shift-and-subtract method. Again, the results are more consistent for the reference pixels.

As illustrated in Figure 4.1, the noise reduction achieved with IRP readout is equivalent to that resulting from the shift-and-subtract technique for both the UMC and the ON H4RG-15 SCA. The small differences may be due to the specific common mode noise rejection achieved by each technique (primarily that the common mode subtracted pixels are read simultaneously with shift-and-subtract but sequentially for IRP readout and that they are read through the same output signal chain – including the ASIC preamplifier and ADC – for IRP readout but through different signal chains for the shift-and-subtract). However at this level they could also be due to the masking of a significant fraction of defective pixels in these Phase-1 H4RG-15 SCAs. They are far too small to have any effect on any decisions as to the Phase-2 program and will be further evaluated using Phase-2 SCAs when they become available.

In IRP readout mode, the swing in signal level jumping from signal to reference pixels is much larger than the swing from one pixel to the next during conventional readout of a typical astronomical image. This requires careful tuning of the ROIC and this has been particularly important for both Phase-1 SCAs due to their high current draw. We were able to achieve good enough performance to adopt IRP readout, with all of its common-mode noise rejection benefits, for all of the observations at the telescope and intend to emphasize optimization of IRP readout in the characterization of Phase-2 SCAs.

5. IMAGING AT THE UH 88-INCH TELESCOPE ON MAUNA KEA

A telescope at a superior site provides the ultimate test facility for the evaluation of astronomical infrared arrays and flexible access to the 88-inch telescope on Mauna Kea is a major strength of the UH Infrared-Optical (IO) sensor array development program. As demonstrated during the JWST H2RG development program, ULBCam's telescope configuration takes full advantage of this. At 0.2 arc-seconds per pixel for the 15 μm pixel H4RG-15, it provides a 14 x 14 arc-minute field with sub arc-second imaging. Standard astronomical Z, J and H filters are standard with the option of replacing any of them with custom filters for specific tests or observations. A UH 88-inch telescope imaging run with the H4RG-15 SCA installed in ULBCam provides the ultimate end-to-end test of SCA performance and is the centerpiece of the UH Phase-1 program. On the basis of the UH laboratory characterization, both the UMC and ON H4RG-15 SCAs fully qualified for further evaluation at the telescope. However schedule and cost constraints allowed only one SCA to be evaluated at the telescope and, based on factors other than the laboratory test results (primarily the extensive experience with UMC H2RGs at a wide range of telescopes), the ON H4RG-15 SCA was selected.

It was scheduled for two bright half nights around full moon (May 4 and 5) followed by a single full night May 7 with several contingency nights scheduled around each of the next two full moons. These were not required as ULBCam with the ON H4RG-15 SCA installed was brought into full astronomical operation during the first two half nights and the full night of May 7 was used to successfully execute the entire commissioning program at the telescope. Full 13 pointing "dither" sequences were observed in both J and H spectral bands, along with companion blank fields and the usual darks and flats, for Messier 51 (the Whirlpool Galaxy), the Hubble Deep Field North and the Galactic star forming region Serpens South. The June and July nights were returned to the pool and ULBCam was returned to the IfA Hilo lab. The Messier 51 observations have been reduced to corrected, calibrated J and H band images. Despite some challenges and limitations associated with the high current draw and the optimization of the IRP readout as the well is filled, the resulting images as shown in Figures 5.1a and b (higher quality versions are available at <http://www.ifa.hawaii.edu/info/press-releases/H4RG-15/>) confirm the superb imaging performance of this H4RG-15 SCA.

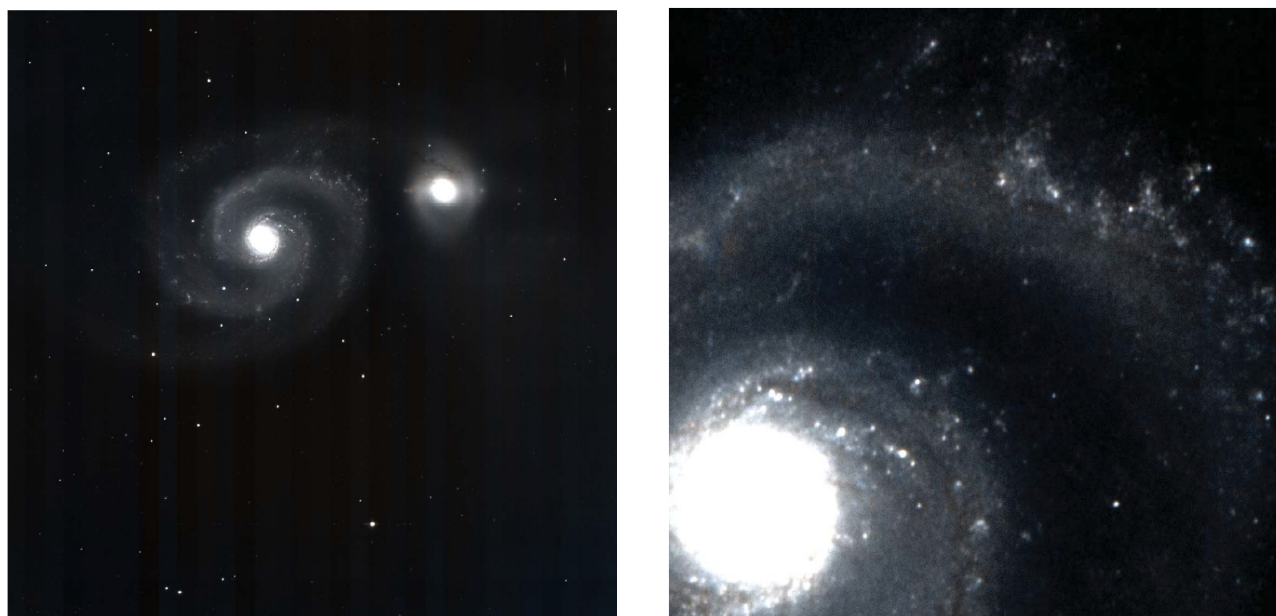


Figure 5.1: First light pictures from the H4RG-15 via ULBCam at the UH 88-inch telescope on Mauna Kea.

6. CONCLUSIONS

In the six months since the ON SCA was first installed, the UH Phase-1 H4RG-15 laboratory test program has achieved all of its primary goals by: 1) verifying that a UMC H4RG-15 SCA maintains the performance of the H2RG, particularly with regard to CDS read noise, 2) demonstrating that an ON H4RG-15 SCA at least matches this performance at the

required cryogenic temperatures and, 3) confirming the functionality and advantages of features new to the H4RG-15, notably the clocked reference output and IRP readout. Imaging with the ON H4RG-15 SCA at the UH 88-inch telescope on Mauna Kea has further provided end-to-end verification of the performance of this array in actual astronomical observations. Together these successfully close out the overall objectives of the UH Phase-1 test program, opening the way for the Phase-2 program to proceed on schedule.

ACKNOWLEDGEMENTS

The authors wish to acknowledge the support of both the NASA NAS 2-98077 "Development of Advanced Near Infrared Focal Plane Technology for Origins / Next Generation Space Telescope", 8/01/1998 through 9/22/2003, and, currently, NSF Advanced Technology and Instrumentation (ATI) award No.AST-0804651: "Development of the H4RG-15; A Low Cost, High Performance 4096x4096 pixel Array for Infrared Astronomy and the Building Block for Very Large IR Mosaic Focal Planes", 10/01/2009 through 9/30/2013.

REFERENCES

- [1] Blank, Richard, Beletic, James W., Cooper, Donald, Farris, Mark, Hall, Donald N. B., Hodapp, Klaus W., Luppino, Gerard, Piquette, Eric and Xu, Min. **"Development and Production of the H4RG-15 Focal Plane Array"**, Proc. SPIE 8543, 854332 (2012).
- [2] Hall, Donald N.B., and Luppino, G., Hodapp, K.W., Garnett, J., Loose, M and Zandian, M. **"A 4K x 4K HgCdTe astronomical camera enabled by the James Webb Space Telescope NIR detector development program"** (invited), Optical and Infrared Detectors for Astronomy, Proc. SPIE, 5499, 1 – 14 (2004).
- [3] Hall, Donald N.B., Hodapp, K.W., Goldsmith, D.L., Cabelli, C., Haas, A.K., Kozlowski, L.J. and Vural, K. **"Characterization of $\lambda c \sim 5\mu m$ Hg: Cd: Te arrays for low-background astronomy"**, Optical and IR Telescope Instrumentation and Detectors, Proc. SPIE, 4008, 1268-1279 (2000).
- [4] Gert Finger, Reinhold J. Dorn, Siegfried Eschbaumer, Donald N. B. Hall, Leander, Mehrgan, Manfred Meyer, and Joerg Stegmeier. **"Performance evaluation, readout modes, and calibration techniques of HgCdTe Hawaii-2RG mosaic arrays"**. Proc. SPIE 7021, 70210P (2008).
- [5] Smith, Roger, Bebek, Christopher, Bonati, Marco, Brown, Matthew D., Cole, Daqvid, Rahmer, Gustavo, Schubell, Michael, Seshadri, Suresh and Tarle, Gregory. **"Noise and zero point drift in 1.7 μm cutoff detectors for SNAP"** Proc. SPIE 6276, 627630 (2006).
- [6] Hall, Donald N. B., NASA contract No.AST-0804651: **"Development of the H4RG-15; A Low Cost, High Performance 4096x4096 pixel Array for Infrared Astronomy and the Building Block for Very Large IR Mosaic Focal Planes"** Final report (2006).
- [7] Rauscher, Bernard j., Arendt, Richard G., Fixsen, Dale J., Lindler, Don J., Loose, Markus, Lander, Matthew, Moseley, Samuel H. and Wilson, Donna V. **"Reducing the read noise of near-infrared detector systems by improved reference sampling and subtraction"** Proc. SPIE 8453, 845351 (2012).